Pis'ma v ZhETF

Magnetic ground state and multiferroicity in $BiMnO_3$

I. V. Solovyev[+*1)], *Z. V. Pchelkina*[*2)]

[+]*Computational Materials Science Center, National Institute for Materials Science, 1-2-1 Sengen, Tsukuba, Ibaraki 305-0047, Japan*

[*]*Institute of Metal Physics, Russian Academy of Sciences-Ural Division, 620041 Yekaterinburg GSP-170, Russia*

Submitted Today

arXiv:0904.0348v1 [cond-mat.mtrl-sci] 2 Apr 2009

We argue that the centrosymmetric $C2/c$ symmetry in $BiMnO_3$ is spontaneously broken by antiferromagnetic (AFM) interactions existing in the system. The true symmetry is expected to be Cc, which is compatible with the noncollinear magnetic ground state, where the ferromagnetic order along one crystallographic axis coexists with the the hidden AFM order *and related to it ferroelectric polarization* along two other axes. The $C2/c$ symmetry can be restored by the magnetic field $B \sim 35$ Tesla, which switches off the ferroelectric polarization. Our analysis is based on the solution of the low-energy model constructed for the $3d$-bands of $BiMnO_3$, where all the parameters have been derived from the first-principles calculations. Test calculations for isostructural $BiCrO_3$ reveal an excellent agreement with experimental data.

PACS: 75.25.+z, 77.80.-e, 75.30.-m, 71.10.Fd

$BiMnO_3$ is regarded as one of the prominent multiferroic materials, where the ferromagnetic (FM) magnetization is coupled to the ferroelectric polarization, thus, giving a possibility to control the magnetic properties by applying the electric field and vise versa. The ferromagnetism of $BiMnO_3$ is well established today: the Curie temperature is about 100 K and the largest reported magnetization is 3.92 μ_B per formula unit [1], which is close to 4 μ_B expected for the fully saturated FM state. The ferroelectric hysteresis loop was also observed in polycrystalline and thin film samples of $BiMnO_3$ [2], although the measured polarization was small (about 0.043 μC/cm^2). The multiferroic behavior of $BiMnO_3$ is typically attributed to the existence of two different sublattices: the stereochemical activity of Bi($6s^2$) lone pairs is believed to be the origin of the structural distortions (having the $C2$ symmetry) and the inversion symmetry breaking, which gives rise to the ferroelectricity, while the Mn-sublattice is responsible for the magnetism [3]. This point of view dominated over several years and was documented in many review articles [4].

Nevertheless, in 2007 Belik *et al.* have reexamined the crystal structure of $BiMnO_3$ and argued that below 770 K, it is best described by the space group $C2/c$, which has the inversion symmetry [1]. This finding was later confirmed by Montanari *et al.* [5]. According to this new crystal structure information, $BiMnO_3$ can be only in an *antiferroelectric* state [6] – the situation, which is rather common for many distorted perovskites and hardly interesting from the practical point of view. Of course, these experimental works raised many questions. Particularly, what is the origin of the inversion symmetry breaking (if any) and ferroelectric response in $BiMnO_3$?

In our previous work, we have constructed an effective Hubbard-type model for the $3d$-bands of $BiMnO_3$ located near the Fermi level [7]. All parameters of this model were derived in an *ab initio* fashion on the basis of first-principles electronic structure calculations and, apart from approximations inherent to the construction of the low-energy model [8, 9], no adjustable parameters have been used. Then, from the solution of this model in the mean-field Hartree-Fock (HF) approximation we derived parameters of interatomic magnetic interactions and argued that, in the $C2/c$ structure, the nearest-neighbor FM interactions (J_{NN}) compete with the longer range antiferromagnetic (AFM) interactions (J_{LR}, see Fig.1). The latter make the sites 1 and 2 inequivalent and tend to break the inversion center located in the midpoint of the cube diagonal connecting these two sites. Both interactions are directly related to the orbital ordering realized in $BiMnO_3$ below 550 K. This suggests that the ferroelectric behavior of $BiMnO_3$ could be related to some hidden AFM order, which is driven by J_{LR} and which in [7] was denoted as the $\uparrow\downarrow\downarrow\uparrow$ order, referring to the directions of spins at four Mn-atoms in the primitive cell. But, now we face a more fundamental problem: how to reconcile the AFM structure, which is needed in order to break the inversion symmetry, with the FM behavior of $BiMnO_3$, which is clearly seen in the experiment?

1) e-mail: SOLOVYEV.Igor@nims.go.jp
2) e-mail: pzv@ifmlrs.uran.ru

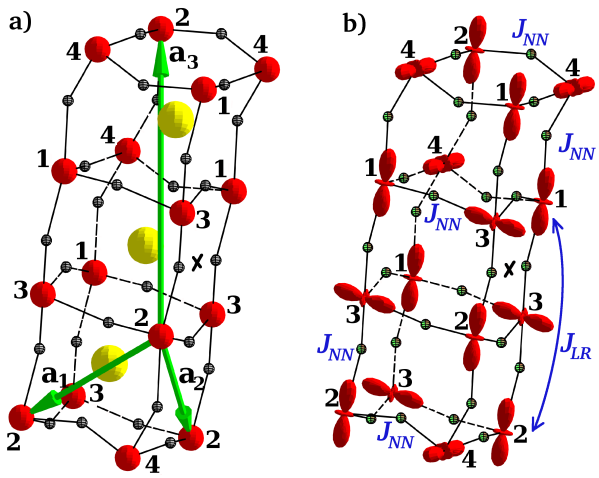

Fig.1. (a) Crystal structure of $BiMnO_3$. Bi-, Mn-, and O-atoms are indicated by big, medium, and small spheres, respectively. Primitive translations are shown by arrows. Four Mn-atoms, composing the primitive cell of $BiMnO_3$, are indicated by numbers. (b) Distribution of charge densities associated with the occupied e_g orbitals (the orbital ordering) realized in the low-temperature phase of $BiMnO_3$ and related to it nearest-neighbor ferromagnetic (J_{NN}) and longer range antiferromagnetic (J_{LR}) interactions. The position of the inversion center in the $C2/c$ structure is marked by the cross.

The clue to this problem may be related to the quasi-degeneracy of the FM and ↑↓↓↑ AFM states. Indeed, according to the HF calculations, the total energy difference between these two states was only 0.5 meV per one formula unit [7]. Although the value itself maybe at the edge of accuracy of the model calculations, it gives a clear ideas about characteristic energy scale we have to deal with in the process of analysis of the magnetic properties of $BiMnO_3$.

In the present work we further develop this idea and argue that the AFM ↑↓↓↑ and FM states can be easily mixed by the relativistic spin-orbit (SO) interaction $\xi\hat{\mathbf{s}}\cdot\hat{\mathbf{l}}$. Although the expectation value of the orbital magnetic moment $\mu_B\hat{\mathbf{l}}$ is small in manganites (typically, few hundredths of μ_B [10]), the constant of the SO interaction ξ is about 50 meV. Thus, the energy gain caused by the SO interaction can become comparable with the total energy difference between the FM and ↑↓↓↑ AFM states. First, using general symmetry considerations, we argue that the true magnetic ground state of $BiMnO_3$ is noncollinear and includes both FM and AFM components of the magnetic moments. This naturally resolves the puzzle of multiferroicity of $BiMnO_3$: the inversion symmetry is broken by the hidden AFM order, while the FM component appears due to the canting of the magnetic moments. The idea will be further supported by the direct optimization of the magnetic structure of $BiMnO_3$ in the model HF calculations with the SO interaction. Finally, we show how the ferroelectric polarization can be controlled by the external magnetic field, which acts on the FM component of the magnetic moments. Particularly, we predict the existence of the critical field B_c, which restores the inversion symmetry and switches off the ferroelectric polarization.

We begin with the symmetry considerations. The space group $C2/c$ has four symmetry operations: $\hat{S}_1{=}\hat{E}$, $\hat{S}_2{=}\hat{I}$, $\hat{S}_3{=}\{\hat{m}_y|\mathbf{a}_3/2\}$, $\hat{S}_4{=}\{\hat{C}^2_y|\mathbf{a}_3/2\}$, where $\hat{E}$ is the unity, $\hat{I}$ is the inversion, $\hat{m}_y$ is the mirror reflection of the y-axis, and $\hat{C}^2_y$ is the 180° rotation around the y-axis. The last two operations are combined with the translation by the vector $\mathbf{a}_3/2$ (see Fig.1a). The directions of x, y, and z are related to the directions of the primitive translations as follows: $x\|(\mathbf{a}_1{+}\mathbf{a}_2{+}0.34\mathbf{a}_3)$, $y\|(\mathbf{a}_2{-}\mathbf{a}_1)$, and $z\|\mathbf{a}_3$. Four Mn-atoms are divided in two classes: (1,2) and (3,4). Atoms of one class are transformed by the symmetry operations only to each other, but not to atoms of another class. The magnetic groups corresponding to the $C2/c$ space group are obtained by combining the symmetry operations $\hat{S}_2$-$\hat{S}_4$ with the time inversion $\hat{T}$, which additionally flips the directions of the magnetic moments. Then, there are two magnetic groups, which can be regarded as candidates for the magnetic ground state of $BiMnO_3$: $\mathbf{G}_1{=}\{\hat{S}_1,\hat{S}_2,\hat{S}_3,\hat{S}_4\}$ and $\mathbf{G}_2{=}\{\hat{S}_1,\hat{S}_2,\hat{S}_3\hat{T},\hat{S}_4\hat{T}\}$. The third possibility includes the symmetry operation $\hat{S}_2\hat{T}{\equiv}\hat{I}\hat{T}$. However, since $\hat{I}$ transforms the atoms 3 and 4 to themselves, the symmetry operation $\hat{I}\hat{T}$ corresponds to the non-magnetic sublattice (3,4). Such a situation, although formally possible, cannot be realized as the magnetic ground state of $BiMnO_3$, because it contradicts to the first Hund rule [7]. Then, x and z projections of the magnetic moments obey the same transformation rules under the symmetry operations $\hat{S}_1$-$\hat{S}_4$. Therefore, the magnetic structure of $BiMnO_3$ can be generally abbreviated as $\mathcal{AB}$-$\mathcal{CD}$, where each capital letter stands for the magnetic arrangement (ferromagnetic - F, antiferromagnetic - A, or with zero projection of the magnetic moment - Z) formed by the x and y projections of the magnetic moments of the atoms (1,2) and (3,4): first two capital letters describe the magnetic arrangement in the pair (1,2) formed by the x ($\mathcal{A}$) and y ($\mathcal{B}$) projections of the magnetic moments; while second two capital letters describe the magnetic arrangement in the pair (3,4) formed by the x ($\mathcal{C}$) and y ($\mathcal{D}$) projections of the magnetic moments. For example, the magnetic structure corresponding to $\mathbf{G}_1$ and $\mathbf{G}_2$ can be denoted as ZF-AF

and FZ-FA, respectively. Moreover, we consider the solutions with the spontaneous symmetry breaking corresponding to three possible subgroups of the space group $C2/c$. From this point of view, the most promising are two magnetic subgroups: $\mathbf{G}_3=\{\hat{S}_1, \hat{S}_3\}$ (the space group Cc, No. 9 in International Tables) and $\mathbf{G}_4=\{\hat{S}_1, \hat{S}_3\hat{T}\}$, which preserve the atomic classes (1,2) and (3,4). They correspond to the magnetic structures AF-AF and FA-FA, respectively. In the other words, contrary to $\mathbf{G}_1$ and $\mathbf{G}_2$, the magnetic subgroups $\mathbf{G}_3$ and $\mathbf{G}_4$ allow for the nontrivial AFM arrangement in the pair (1,2) with finite projections of the magnetic moments. Such a situation becomes possible due to the breaking of the inversion symmetry $\hat{I}$ (relative to the center, which is shown by the cross in Fig.1b). In the case of the collinear magnetic arrangement, the magnetic structures AF-AF and FA-FA are reduced to either FM or AFM $\uparrow\downarrow\downarrow\uparrow$ ones, which have been considered in [7] without the SO interaction. Other magnetic subgroups, generated by $\hat{S}_2=\hat{I}$ and $\hat{S}_4=\{\hat{C}_y^2|\mathbf{a}_3/2\}$ destroy the atomic classes and make the atoms forming the pairs (1,2) and (3,4) inequivalent. Although such solutions are formally possible, all of them are unstable and not realized as the magnetic ground state of $BiMnO_3$, as it will become clear from the solution of the low-energy model.

Our next goal is the search for the true (and so far unknown) magnetic ground state of $BiMnO_3$ based on the solution of the low-energy model. However, before doing any predictions for $BiMnO_3$, we would like to show some test calculations for the isostructural compound $BiCrO_3$ [11], which give some idea about the accuracy of our approach. The formal configuration of Cr^{3+} ions in $BiCrO_3$ is t_{2g}^3. Since the t_{2g}-levels are well separated form the e_g-ones by the crystal-field (CF) effects, the orbital degrees of freedom in $BiCrO_3$ are quenched and the Hubbard model can be further mapped onto the Heisenberg model $\hat{\mathcal{H}}_S = -\sum_{i>j} J_{ij}\hat{\mathbf{S}}_i\hat{\mathbf{S}}_j$ with the spin 3/2.[3)] The parameters of such a model are shown in Fig.2a. Generally, the distribution of the magnetic moments associated with the existence of two inequivalent sublattices (1,2) and (3,4) should be nonuniform. The magnitude of this effect can be estimated in the mean-field approximation. However, it appears that from the magnetic point of view, the sublattices (1,2) and (3,4) are nearly equivalent. Indeed, the behavior of local magnetization at the sites 1 and 3 (Fig.2b) is practically indistinguishable in the whole temperature range below the Néel temperature T_N (about 204 K in the mean-field approximation). Then, a proper (and much better) estimate for T_N can be obtained by assuming that the main excitations in $BiCrO_3$ can be described by (uniform) spin waves and employing the renormalized spin-wave theory, which takes into account the spacial correlations between the spins [12]. It yields T_N=123 K, which is very close to the experimental value T_N=109 K [13].

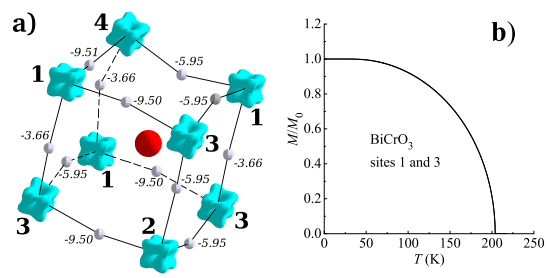

Fig.2. (a) Distribution of occupied t_{2g}-orbitals at the Cr-sites and corresponding parameters of Heisenberg model ($J_{ij}S^2$, where S=3/2) associated with different bonds in $BiCrO_3$. Bi- and O-atoms are shown by big and small spheres, respectively. (b) Corresponding temperature dependence of the local magnetization at the sites 1 and 3 in the mean-field approximation, which demonstrates that the two curves are practically indistinguishable, despite the fact that the sites 1 and 3 are inequivalent and belong to different atomic classes.

Being encouraged by these results, we now turn to the problem of the magnetic ground state and the origin of the ferroelectric behavior of $BiMnO_3$. First, we perform the delicate optimization of the magnetic structure of $BiMnO_3$ based on the HF solution of the low-energy model with the SO interaction. The parameters of the low-energy model were reported in [7]. The solution of the low-energy model with the SO interaction was performed along the same line as for other distorted perovskite oxides considered in the review article [9]. A typical iterative procedure is shown in Fig.3. In this case, we start with the FM solution, where all magnetic moments were aligned along the y-axis, switch on the SO interaction, and monitor the behavior of the FM moments (M_y^1=M_y^2) as well as two AFM order parameters L_x=$(M_x^1-M_x^2)/2$ and L_z=$(M_z^1-M_z^2)/2$, which were developed at the sites 1 and 2 in the process of iterative

[3)] We used the same strategy as in our previous work on $BiMnO_3$ [7]. First, we construct an effective Hubbard-type model. The main difference of the model parameters from the ones reported for $BiMnO_3$ [7] is the following: the CF-splitting between two e_g-levels is small (134 and 185 meV for the sites 1 and 3, respectively), while the t_{2g}-e_g splitting is large (about 2.1 eV). Moreover, the on-site Coulomb repulsion U is larger in $BiCrO_3$: 2.63 and 2.73 eV for the sites 1 and 3, resectively. Then, we calculate J_{ij} using infinitesimal rotations near the $\uparrow\uparrow\downarrow\downarrow$ (or G-type) AFM ground state. In $BiCrO_3$, other magnetic configurations yield practically the same set of the exchange parameters J_{ij}, meaning that the mapping onto the Heisenberg model is universe and does not depend on the magnetic state.

solution of the HF equations. In these notations, M_a^i is the projection of the magnetic moment at the site i parallel to the a-axis, where a= x, y, or z. In the

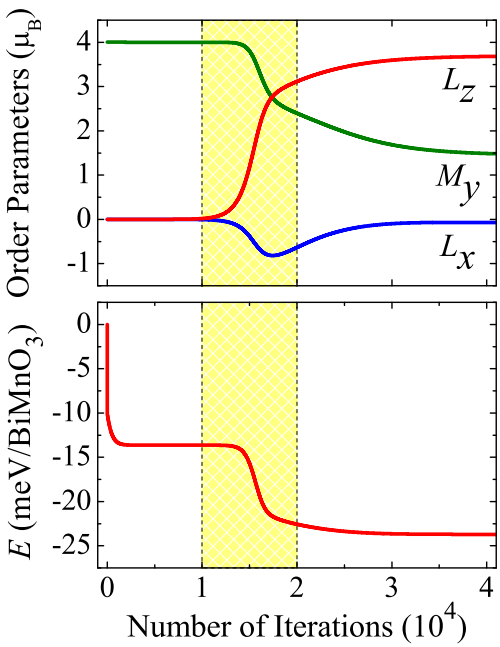

Fig.3. Convergence of the ferromagnetic moment $M_y \equiv M_y^1 = M_y^2$, two antiferromagnetic order parameters $L_x = (M_x^1 - M_x^2)/2$ and $L_z = (M_z^1 - M_z^2)/2$, and the total energy in the Hartree-Fock calculations after switching on the spin-orbit interaction. The initial configuration corresponded to the self-consistent Hartree-Fock solution for the ferromagnetic state without spin-orbit interaction, where all magnetic moments were aligned along the y-axis. The shaded area is the region corresponding to the change of the symmetry $\mathbf{G}_1 \Rightarrow \mathbf{G}_3$ of the Hartree-Fock solution by the antiferromagnetic interactions.

process of first approximately 10^4 iterations, the solution obeys the $\mathbf{G}_1$ symmetry, and the iterative procedure is accompanied by the small but steady decrease of the total energy (following the sharp drop right after switching on the SO interaction). As expected, the x- and z-projections of the magnetic moments at the sites 1 and 2 are exactly equal to zero in this region (so as the AFM order parameters L_x and L_z). However, in the process of next 10^4 iterations we clearly observe the lowering of the magnetic symmetry $\mathbf{G}_1 \Rightarrow \mathbf{G}_3$, which is accompanied by the growth of AFM order parameters L_x and L_z (at the expense of the FM magnetization along y) and the step decrease of the total energy of the system (by about 10 meV per one formula unit). This solution finally converges to the following values of the magnetic moments $\mathbf{M}$=(M_x, M_y, M_z) at the sites 1-4 (in μ_B):

$$\begin{aligned}
\mathbf{M}^1 &= (\ \ 0.08, -1.45, -3.69)\\
\mathbf{M}^2 &= (-0.08, -1.45,\ \ 3.69)\\
\mathbf{M}^3 &= (-0.97, -2.02, -3.27)\\
\mathbf{M}^4 &= (\ \ 0.97, -2.02,\ \ 3.27)
\end{aligned}$$

We also tried to start with other magnetic configurations (including all magnetic configurations considered in [7] with different directions of the magnetic moments). However, all of them finally converged to the solution described above. For example, by starting with the AFM ↑↓↓↑ configuration and aligning all magnetic moments along y-axis, one can obtain a metastable solution having the $\mathbf{G}_2$ symmetry, which is only 3 meV higher that the $\mathbf{G}_3$ solution discussed above. However, even this metastable solution finally converged to the $\mathbf{G}_3$ one, which seems to be the true global minimum of the total energy of the system. These calculations clearly show the advantages of working with the low-energy models, because in order to reach the true global minimum with the SO interaction, we typically need a huge number of iterations, which is only affordable in the model approach.

We would also like to emphasize that the symmetry of the magnetic ground state, obtained in the present work, is incompatible with the noncentrosymmetric crystal structure $C2$, which was proposed in earlier studies [14] and was shown to be unstable [6] with respect to the centrosymmetric $C2/c$ structure [1]. Instead, we propose that, at least below the magnetic transition temperature, the crystal structure of $BiMnO_3$ should have the Cc symmetry. This finding should be checked experimentally and we hope that our work will stimulate further activities in this direction.

The magnetic group $\mathbf{G}_3$ allows for the net electric polarization $\mathbf{P}$ in the plane zx, which is a normal vector and does not changes its sign under $\hat{S}_3$=$\{\hat{m}_y|\mathbf{a}_3/2\}$. On the other hand, $\mathbf{M}$ is an axial vector and both AFM order parameters L_x and L_z change the sign under $\hat{S}_3$. Therefore, the ferroelectric polarization caused by the magnetic degrees of freedom must be at least bilinear with respect to L_x and L_z [15]:

$$P_a = \sum_{bc} \chi_{abc} L_b L_c, \qquad (1)$$

where the symbols a, b, and c denote the z and x projections of the vectors. Since L_x and L_z are related to the the FM magnetization M_y (due to the conservation of $|\mathbf{M}|$), the value of $\mathbf{P}$ can be controlled by the external magnetic field $\mathbf{B}$=$(0, B, 0)$, applied along y and

coupled to M_y. Fig.4 shows results of HF calculations in the external magnetic field. The corresponding interaction term is described by $\hat{\mathcal{H}}_B = -\mu_B \mathbf{B} \cdot (2\hat{\mathbf{s}}+\hat{\mathbf{l}})$. As expected, $\mathbf{B}$ saturates the FM magnetization M_y.

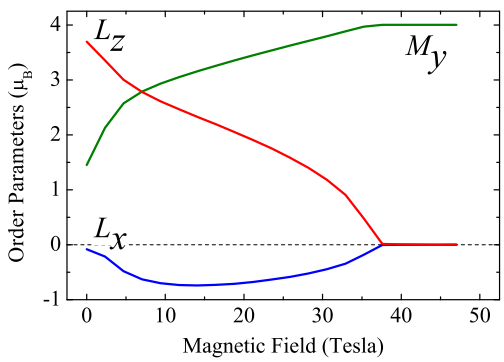

Fig.4. Behavior of the ferromagnetic magnetization $M_y \equiv M_y^1 = M_y^2$ and the antiferromagnetic order parameters $L_x = (M_x^1 - M_x^2)/2$ and $L_z = (M_z^1 - M_z^2)/2$ in the external magnetic field along the y-axis.

Then, other two projections of the magnetic moments will decrease, so as the AFM order parameters L_x and L_z. Therefore, the ferroelectric polarization (1) should also decrease. When the field exceeds some critical value $B_c \sim 35$ Tesla, both L_x and L_z vanish. Thus, $B > B_c$ restores the full symmetry of the system, $\mathbf{G}_3 \Rightarrow \mathbf{G}_1$, and switches off the ferroelectric polarization. This finding is very important for practical applications as it clearly demonstrates how the ferroelectric behavior of $BiMnO_3$ can be controlled by the magnetic field. Of course, the obtained B_c is too large for any practical applications. Nevertheless, this theoretical value may be overestimated because the model itself does not include several important ingredients such as the magnetic polarization of the oxygen sites [7]. The latter will additionally stabilize the FM interactions [7, 16] and therefore decrease B_c. On the other hand, the FM interactions at the oxygen sites will be partly compensated by AFM interactions, which are additionally stabilized by correlation effects beyond the HF approximation [16]. Moreover, the relative strength of FM and AFM interactions (and therefore B_c) could be tuned by the external factors such as pressure, defects or the lattice mismatch in the thin films of $BiMnO_3$ deposed on different substrates [7].

In conclusion, we predict that the centrosymmetric $C2/c$ symmetry in $BiMnO_3$ is spontaneously broken by hidden AFM interactions, which downgrade the actual symmetry to the Cc one (No. 9 in International Tables). The space group Cc has only one nontrivial symmetry operation (the mirror reflection of the y-axis with subsequent translation by $\mathbf{a}_3/2$), which allows for the existence of both ferromagnetic order (along the y-axis) and ferroelectric polarization (in the plane perpendicular to y). The full $C2/c$ symmetry can be restored in the external magnetic field, which can be used in practical applications in order to completely switch off the ferroelectric polarization.

The work of IVS is partly supported by Grant-in-Aid for Scientific Research in Priority Area "Anomalous Quantum Materials" and Grant-in-Aid for Scientific Research (C) No. 20540337 from the Ministry of Education, Culture, Sport, Science and Technology of Japan. The work of ZVP is partly supported by Dynasty Foundation, Grants of President of Russia MK-3227.2008.2, and scientific school grant SS-1929.2008.2.

REFERENCES

1. A. A. Belik, S. Iikubo, T. Yokosawa, et al., J. Am. Cham. Soc. **129**, 971 (2007).
2. A. Moreira dos Santos, S. Parashar, A. R. Raju, et al., Solid State Commun. **122**, 49 (2002).
3. R. Seshadri and N. A. Hill, Chem. Mater. **13**, 2892 (2001).
4. S.-W. Cheong and M. Mostovoy, Nature materials **6**, 13 (2007).
5. E. Montanari, G. Calestani, L. Righi, et al., Phys. Rev. B **75**, 220101(R) (2007).
6. P. Baettig, R. Seshadri and N. A. Spaldin, J. Am. Chem. Soc. **129**, 9854 (2007).
7. I. V. Solovyev and Z. V. Pchelkina, New J. Phys. **10**, 073021 (2008).
8. I. V. Solovyev, Phys. Rev. B **73**, 155117 (2006).
9. I. V. Solovyev, J. Phys.: Condens. Matter **20**, 293201 (2008).
10. I. Solovyev, N. Hamada and K. Terakura, Phys. Rev. Lett. **76**, 4825 (1996).
11. A. A. Belik, S. Iikubo, K. Kodama, et al., Chem. Mater. **20**, 3765 (2008).
12. S. V. Tyablikov, in: *Methods of Quantum Theory of Magnetism*, Moscow: Nauka, 1975.
13. A. A. Belik, N. Tsujii, H. Suzuki, and E. Takayama-Muromachi, Inorg. Chem. **46**, 8746 (2007).
14. T. Atou, H. Chiba, K. Ohoyama, et al., J. Solid State Chem. **145**, 639 (1999).
15. G. A. Smolenskii and I. E. Chupis, Usp. Fiz. Nauk **137**, 415 (1982).
16. I. Solovyev, J. Phys. Soc. Jpn. (accepted for publication) (2009), arXiv:0812.3191.